

# Duty-cycle passive time characterisation for input power and energy storage variation of an energy harvesting tailored wireless sensing system

V Marsic<sup>1</sup>, M Zhu<sup>2</sup>

<sup>1</sup> Manufacturing and Materials Department, Cranfield University, Bedfordshire, MK43 0AL, UK.

<sup>2</sup> College of Engineering, Mathematics and Physical Sciences, Exeter University, Devon, EX4 4SB, UK.

E-mail: m.zhu@exeter.ac.uk

**Abstract.** This experimental study investigates the duty-cycle passive times modifications for a low power wireless sensing system (WSS) designed for energy harvesting technology when its input power level and energy storage size are varying. The different low power WSSs presented in the literature feature specific designs aimed at solving particular problems, and due to their specificity their performance indicators are not directly comparable. As a result of this incompatibility, one cannot identify a correlation between the input power, energy storage element size, passive and active time variations to evaluate the potential usability of the system for static or dynamic testing. The present work covers this result comparison gap induced by the incompatibility factor, providing the experimental data obtained as a result of input power level and energy storage size variation for the same low power WSS, thus generating a reference point for the advanced designer and also for the inexperienced user. The experimental results illustrate that, by varying the storage capacity of a low power WSS, its input power range can be enlarged by up to 20 times.

## 1. Introduction

This study focuses on a low power WSS designed to be autonomous using energy harvesting technology and provides an experimental investigation of its performance when modifying its input power level and energy storage capacity. As the diagram from figure 1 illustrates, the general structure for all applications designed to be powered by an energy harvester (EH) is similar at the block level, the differentiation being made at the component level, [1]:

- EH size, shape, material, energy conversion efficiency and excitation (e.g., light, wind speed, vibration, temperature, etc.) determine the electricity input power level provided to the system.
- Switch A can be a diode rectifying bridge, an alternative current (AC) to direct current (DC) or DC-DC converter, a mechanical or electrical switch designed to convert the EH input power to DC and/or buffer it by boosting, lowering and impedance matching the internal structure of the EH.

<sup>2</sup> To whom any correspondence should be addressed.



- The energy storage element, which can be a capacitor, super-capacitor or a rechargeable battery, can vary in size according to its intended functionality: immediate energy transfer to the WSS when there is enough energy available for one functioning duty-cycle, or long term energy storage in order to facilitate a timed complex operation.
- Switch B can serve the same purposes and functionality as Switch A, plus the capability of keeping the WSS disconnected while the energy storage element is charging, and reconnecting it when enough energy is stored to perform the sensor reading, local data processing and transmitting. The usual circuit used for Switch B is an operational amplifier comparator with hysteresis or a voltage supervisor.
- The wireless sensing system can also vary from the low power radio frequency identification (RFID) architecture transmitting on industrial, scientific and medical (ISM) radio bands, to the ones designed for standard communication protocols like IEEE 802.15.4, ZigBee, Bluetooth, etc.

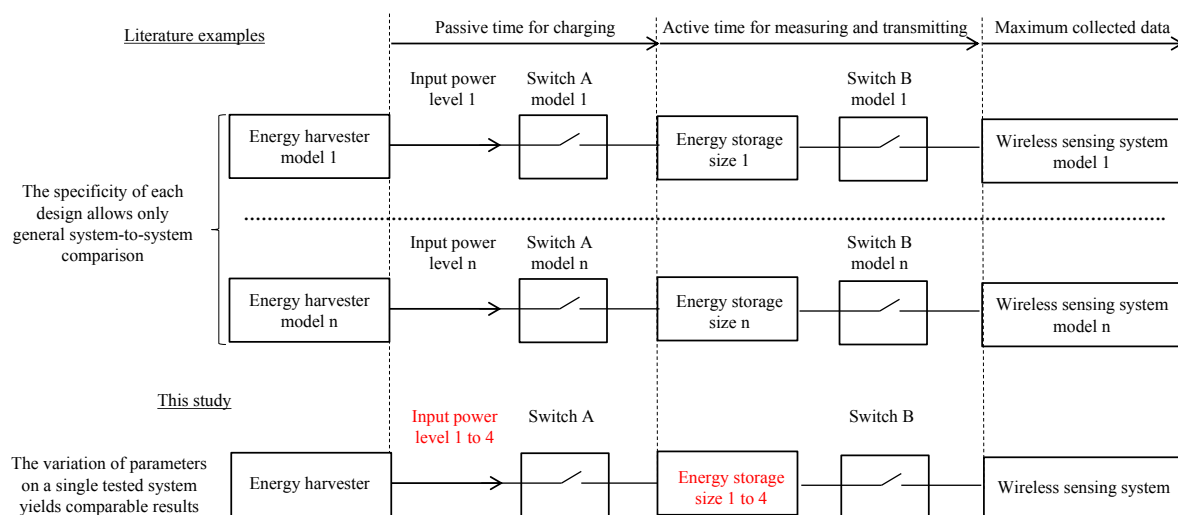


**Figure 1.** Diagram of the general architecture for a low power WSS powered by an energy harvester showing the advantage of a study that characterises the duty-cycle passive time when parameters like input power and energy storage vary

This study, by applying the already acknowledged methodology from prior investigations [2-4] for measuring the passive times for low power wireless communication modules, determines the trend of WSS characteristics resulted from input power level and energy storage size modification. This trend is hard to be spotted because of the large technology variation used in autonomous WSS implementations. Therefore, the findings of this work give an instant lead to future designers and nevertheless to undecided potential users.

## 2. WSS description

The WSS supporting this research has been implemented as previously described in [5], its general internal diagram in connection with the piezoelectric vibration EH being showed in figure 2. The vibration EH uses a thin piezoelectric macro fibre composite (MFC) patented by NASA which is bonded to an aeronautic aluminium alloy plate used as substrate. The MFC is an M8528-P2 rectangular model, commercialised by Smart Material Corporation. Its overall dimensions are 60mm x 103mm, active area being 28mm x 85mm. The active area is made from rectangular piezo-ceramic rods embedded in an epoxy matrix resin along with electrodes and polyimide film. By bonding the MFC on an aeronautical grade substrate, the EH successfully demonstrates in laboratory testing its

potential usage to harvest the strain energy resulted at low frequencies during the flight of an aircraft. This harvested energy could power the WSS to perform structural health monitoring (SHM), [6].

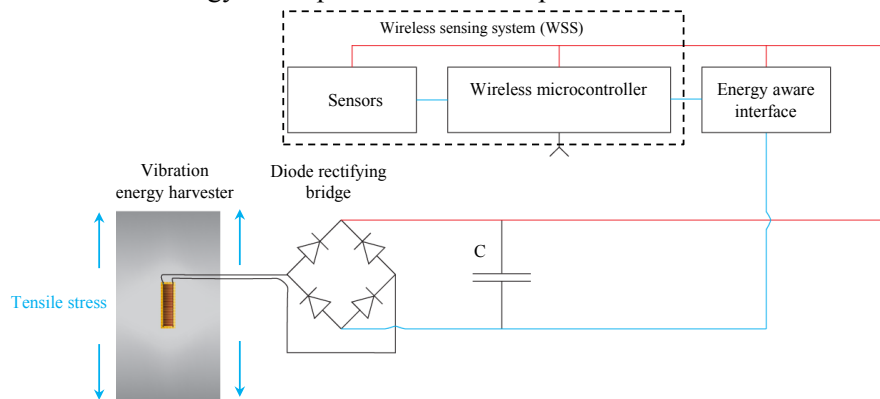


**Figure 2.** General architectural design for the implemented WSS powered by an EH based on a low frequency vibration MFC attached to an aluminium alloy substrate.

The Switch A, presented in figure 1, is implemented as a full wave diode rectifying bridge, therefore reducing the complexity of the circuit and transforming the AC produced by the vibration EH into DC in order to directly charge the energy storage element.

The energy storage element is implemented as an electrolytic capacitor, whose capacitance will be modified to take the values of 1, 2, 5 and 10mF. The minimum value for the electrolytic capacitor is chosen by design to provide enough energy for the WSS to perform its functions.

The Switch B is represented by the energy aware interface (EAI). The EAI monitors the voltage from the storage capacitor and acts as a voltage supervisor with two voltage thresholds. One of the thresholds, when reached during the charging of the storage capacitor, is used to connect the WSS to its ground terminal by the mediation of a 2N7000 N-MOS transistor. The other threshold value attained during the discharge of the storage capacitor due to WSS power consumption, is used to disconnect the WSS ground terminal by commanding the same N-MOS transistor. The EAI, by disconnecting the WSS, allows the energy to be regenerated in the capacitor, and, by connecting the WSS, allows the energy to be used for sensor readings, local data processing and wireless transmission of information in IEEE 802.15.4 data frame format. The voltage threshold chosen by circuit design for the EAI to connect the WSS is  $\sim 3.2\text{V}$  and the second threshold, for disconnecting the WSS, is  $\sim 3.08\text{V}$ .

The wireless sensing system is composed of two blocks. One is the wireless microcontroller, which manages the information between the external sensors and the internal wireless 2.4GHz transceiver. The other block is represented by the sensors. The sensors implemented in the WSS were chosen to have low power consumption and a fast initialisation time. In order to acquire a broad range of data useful for future aeronautical SHM implementation, a 3-axis accelerometer, a temperature and a light intensity sensor were included. Figure 3 shows the resulting prototype system. The full-wave rectifying diode bridge built from four fast switching 1N4148 diodes provides DC to the capacitor

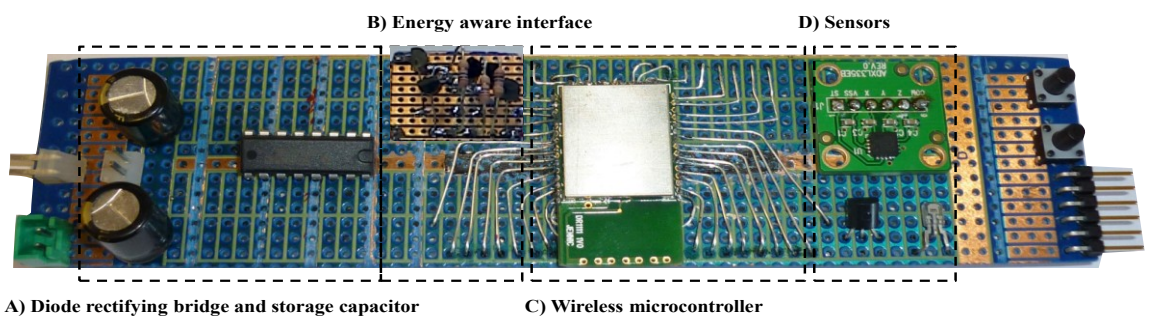


**Figure 3.** Tested wireless sensing system divided into its four distinct areas: (A) and (B) form the power management block, (C) JN5148 wireless microcontroller linking wirelessly the data collected from the sensor block (D) to the beneficiary user base station.

bank composed of two 1mF electrolytic capacitors. The EAI circuit, present on the back of the illustrated module, connects and disconnects the wireless microcontroller from its ground terminal by constantly monitoring the voltage on the capacitor bank. The ultra-low power consumption wireless microcontroller implemented with JN5148 from Jennic-NXP is IEEE 802.15.4/ZigBee-compliant. The wireless microcontroller manages the three external low power analogic sensors: a temperature sensor MCP9700, a 3-axis acceleration sensor ADXL335 and a light intensity sensor GA1A2S100LY.

### 3. WSS testing set-up

The data resulted from measuring the WSS passive times, cold start,  $t_c$ , and warm start,  $t_w$ , are experimentally examined. The diagram set-up illustrated in figure 4 was used for measuring the WSS passive time periods,  $t_c$ , and  $t_w$ . The Agilent 34410A multimeter monitors the voltage on the storage capacitor C, saving the time and voltage measurement data in a comma separated values (CSV) text file format on the computer it is connected to via USB.

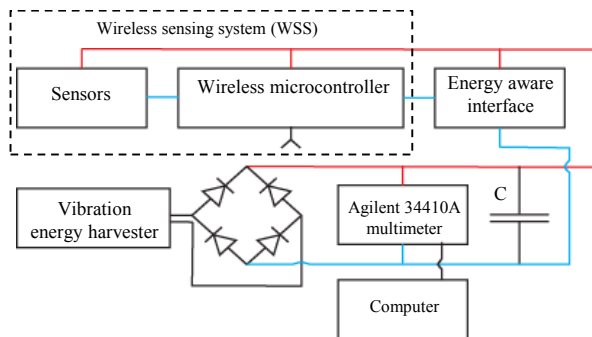


**Figure 4.** Testing set-up for measuring the passive times, cold and warm start of the wireless sensing system.

### 4. Results and discussion

The WSS cold start,  $t_c$ , is produced once at the beginning of the WSS duty-cycle. With the WSS disconnected by the EAI from the storage capacitor C and neglecting the small amount of current required by the EAI to function,  $\sim 1.19\mu\text{A}$ ,  $t_c$  represents a classic case of the time required by the capacitor to charge from level zero to a predefined value (in our case  $\sim 3.2\text{V}$ ). The WSS cold start depends only on the input power value,  $P_{IN}$  and the storage capacitor size. Table 1 presents the values obtained for the WSS cold start by varying the storage capacitor size for a  $10\text{mW}$   $P_{IN}$ , using the testing set-up from figure 4. The EH variation of  $P_{IN}$  is derived from the controlled frequency shift and strain deformation on the MFC based EH aluminium substrate plate produced by the user input data in accordance with real flight vibration scenarios [7]. The corresponding warm start values  $t_w$  are shown in the same table because they also vary in accordance with the power input applied to different size capacitors.

The WSS warm start  $t_w$  has a double significance:

- The time gap between two consecutive wireless data transmissions.
- The charging time for the storage capacitor C, until reaching the pre-set energy threshold validated by the EAI.

In order to analyse the effect of  $P_{IN}$  variation on the WSS warm start,  $t_w$ , the MFC based EH was subjected to the same procedure as the one described above for the cold start  $t_c$  measurements. The DC power source was used to provide the following input powers: 0.5, 1, 5 and  $10\text{mW}$  for the WSS  $2\text{mF}$  capacitor. The results are plotted in figure 5.

**Table 1.** The WSS cold and warm start measured at  $10\text{mW}$  input power when transmitting 20 bytes (10 bytes of data payload and 10 bytes for network addressing, error check, etc.) on  $2.4\text{GHz}$  using IEEE 802.15.4 and a current consumption of  $1.19\mu\text{A}$  for all passive time duration.

C (mF)	$t_c$ (s)	$t_w$ (s)
1	5	0.3
2	9.6	0.4
5	24.3	0.9
10	43.2	1.8

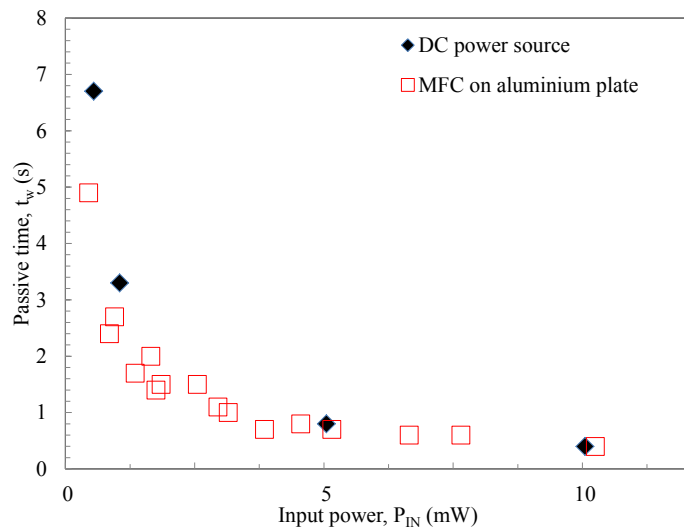


**Figure 5.** The time gap between two consecutive data transmissions (passive time warm start,  $t_w$ ) is plotted against the variable input power provided by an MFC based vibration energy harvester (EH), and by a DC power source being used as a plotting reference for 0.5, 1, 5 and 10mW due to the wide power range generated by the EH due to the frequency and stress inputted by the tensile testing machine.

The impedance mismatch between the EH and the storage capacitor is reflected also in the WSS warm start: the vibration harvester with a maximum produced input power  $P_{IN}$  of 12.16mW measured with a resistive matching load of 66k $\Omega$ , [8], generates a  $t_w$  value similar to the one produced by the DC power source with a  $P_{IN}$  at 10mW. The values presented in table 1 and figure 5 recorded for the same WSS indicate that a low power WSS is functionally adaptive for a broad range of input powers directly correlated with its storage capacity. Considering that the basic functionality of the WSS involves an input power of 0.5mW generated by the EH, by varying only the storage capacity the input power can reach 10mW which represents an enlargement by up to 20 times in the WSS functioning range (implying a similar increase in the amount of data that can be transmitted). By increasing the input power and preserving a fixed storage capacity, the passive times  $t_c$  and  $t_w$  decrease.

## 5. Conclusion

This study has experimentally investigated the duty-cycle passive times modifications for a low power WSS designed for EH technology, and demonstrated that by varying the storage capacity, the WSS input power range can be enlarged by up to 20 times. Also, the speed of consecutive data transmissions gets higher as the input power level is increased and the storage capacity remains fixed.

Further work will be done to synthesise and present by experimental results the implications of input power and storage capacity variation on the active time, energy consumed during a WSS duty-cycle and maximum data amount transmitted given different testing conditions.

## Acknowledgments

The authors acknowledge the support from EPSRC through project SMARTER EP/K017950/1.

## References

- [1] CATRENE Working Group on Energy Autonomous Systems 2009 *Energy Autonomous Systems: Future Trends in Devices, Technology, and Systems* 28 (Belgium: IMEC) pp 1-84
- [2] Casilari E, Jose M, Cano G and Gonzalo C 2010 *J. Sensors* **10** 5443-5468
- [3] Zarrabi H, Al-Khalili A and Savaria Y 2011 *18th IEEE Int. Conf. on El. Circ. and Sys.* 727-731
- [4] Gomez C, Oller J and Paradells J 2012 *J. Sensors* 11734-11753
- [5] Marsic V, Zhu M and Williams S 2012 *J. Telfor* **4** 89 – 94
- [6] Marsic V, Giuliano A, Zhu M 2013 *J. Sensors & Transducers* **18** 156-165
- [7] Pozzi M, Canziani A, Durazo C and Zhu M 2012 *Proc. of SPIE* **8348** 834832–1–10
- [8] Giuliano A, Marsic V, Zhu M 2012 *Proc. IEEE. Int. Conf. iThings* 681-684